Journal of Palaeogeography
2014, 3(3): 309−322
DOI: 10.3724/SP.J.1261.2014.00058

Biopalaeogeography and palaeoecology

Coevality of the sea-level fall and main mass extinction in the Permian−Triassic transition in Xiushui, Jiangxi Province, southern China

Ya-Sheng Wu[1, *], Xiao-Hong Yuan[2], Hong-Xia Jiang[1], Li-Jing Liu[1]

1. Key Laboratory of Petroleum Resources Research, CAS; Institute of Geology and Geophysics, Chinese Academy of Sciences, Beijing 100029, China
2. Research Institute of Petroleum Exploration and Development, PetroChina Huabei Oilfield Company, Cangzhou 062552, China

Abstract A continuous Permian−Triassic boundary (PTB) section has been found and studied for the first time in Xiushui, Jiangxi Province, South China. Evidence for a large sea-level fall has been found in the horizon of 0.8 m below the PTB, from the beginning of *Hindeodus changxingensis* zone (correlatable to *Hindeodus typicalis* Zone of the Meishan section). Sedimentary record indicates that the sea level kept at lowstand, or occasionally rose slowly during the whole *Hindeodus parvus* zone, except another substantial sea-level fall in early *H. parvus* zone. It began a quick rise from the beginning of *Isarcicella staeschei* zone, kept rising for the whole *I. staeschei* zone, and probably caused the stagnation of sea water.

The first severe change in the biota, marked by the sudden disappearance of all stenotropic organisms such as fusulinids and dasycladacians, happened at the same time as the first sea-level fall, and is regarded as the first and main episode of the end-Permian mass extinction in this area. A microbe-dominated biota followed the first extinction, and spanned the late *H. changxingensis* zone and the whole *H. parvus* zone. All the microbes and some other eurytropic organisms including gastropods and ostracods disappeared at the end of the *H. parvus* zone, and the following biota in the *I. staeschei* zone is very simple.

The coevality of the main sea-level fall and the main extinction episode might be causal: both of them might be caused by a drastic climatic cooling.

Key words sea-level fall, mass extinction, Permian−Triassic boundary, end-Permian, climatic cooling, South China

1 Introduction

The biggest biotic crisis of the Phanerozoic occurred in the end of the Permian, and killed more than 90% of marine species, 70% of terrestrial vertebrate genera, most terrestrial plants, 100% of reef-building organisms and reef ecosystems (Wu, 2005a; Wu *et al.*, 2007a, 2007b), and almost all conodonts (Wu, 2005b; Yin *et al.*, 2007). Details about the extinction pattern and the causing mechanism have been one focus of geosciences in the latest two decades (Erwin, 1993; Jin *et al.*, 2000; Krystyn *et al.*, 2003; Weidlich *et al.*, 2003; Adachi *et al.*, 2004; Benton *et al.*, 2004; Twitchett *et al.*, 2004; He, 2005; Xie *et al.*, 2005; Wang *et al.*, 2005a; Wang *et al.*, 2005b; Wu, 2005a; Chen *et al.*, 2006; Shen *et al.*, 2006; Algeo *et al.*, 2007; Feng

* Corresponding author. E-mail: wys@mail.igcas.ac.cn.
Received: 2013−07−19 Accepted: 2013−12−30

et al., 2007; Farabegoli *et al.*, 2007; Kozur, 2007; Yin *et al.*, 2007; Yu *et al.*, 2007; Zhao *et al.*, 2007; Cao *et al.*, 2009; Wu *et al.*, 2010). Environmental changes during the Permian−Triassic transition, such as eustatic sea-level changes, might be responsible for the mass extinction, and has been a key research focus. As to the type and magnitude of the sea-level changes during the P−T transition are concerned, there have been two opposite views. One believed that there was no sea-level fall during the P−T transition (Wignall and Hallam, 1992). The other believed that there was at least one big sea-level fall in the latest end of the Permian (Wu *et al.*, 2003). The dispute is continuing, but, there are more and more reports of evidence favoring the latter (Wu *et al.*, 2006a, 2006b; Jiang and Wu, 2007a, 2007b; Ezaki *et al.*, 2008; Wu *et al.*, 2010; Kershaw *et al.*, 2007, 2012; Wang *et al.*, 2012).

The end-Permian mass extinction has been revealed to include more than one episode (Yin *et al.*, 2007; Wu *et al.*, 2007a, 2007b), and the first episode is the biggest and main one. However, many questions remain to be resolved. The most important and difficult one is what had triggered the main mass extinction episode, and what is responsible for the other extinction episodes. Though extreme oceanic and climate changes caused by massive release of thermogenic carbon dioxide and methane has been proposed as the main possible causing factor (Shen *et al.*, 2011), other causes for the main extinction could not be excluded.

Sea-level changes and mass extinction need to be studied in continuous sections. Most good P−T boundary (PTB) sections are situated in south China, including Sichuan and Guizhou Provinces and Guangxi Zhuang Autonomous Region. In recent years, through manual digging, we have found a good, continuous PTB section in Xiushui, Jiangxi Province, South China. It is near to the section studied by Zhu *et al.* (1994) and Wang *et al.* (2005b). Zhu *et al.* (1994) have studied the conodonts in their section, and Wang *et al.* (2005b) reported the presence of a speckled microbialite layer in that section. The current study on our section has revealed the coevality of the sea-level change and the main mass extinction episode in the P−T transition.

2 Geological settings and features of the Xiushui section

2.1 General geology

The PTB section studied in this paper is exposed about 500 m southwest of Dongling, a small village near Sidu town in Xiushui, Jiangxi Province, South China. Xiushui is about 120 km northwest of Nanchang, the capital of Jiangxi Province. Sedimentological study by Xu *et al.* (1997) revealed that this area was a carbonate platform during the Permian. Reef facies developed in this area in the early and middle period of the latest Permian Changhsingian Stage. Examination of outcrops and labs revealed framestone of reef-core facies built by calcareous sponges. The matrix of the framestone is micritic, indicating that the wave energy on the reef was not strong. The water depth on the reef was not deep, but probably exceeded 20 m, since the reef was below wave base as evidenced by the micritic matrix. In the late Changhsingian Stage, reef ceased growing, and the sedimentary environments changed to an open carbonate platform. After the deposition of about 42-m-thick packstone and wackestone, the water shallowed, and about 33-m-thick spar-cemented skeletal grainstone deposited (Zhu *et al.*, 1994). The skeletal grainstone was massive, containing typical Upper Permian fossils such as fusulinids, calcareous algae, and foraminifer *Colaniella*, and was overlain by 1.5-m-thick medium-bedded speckled rock, which is similar to that described by Wang *et al.* (2005b) from Tiandong, Guangxi. The speckled rock is overlain by 0.5-m-thick dendroid rock. Dendroid microbialites have been reported from Sichuan, Hubei, and many other places, but for the first time from this area. The overlying rock is a thin− to med-bedded grayish micritic limestone without macro− fossils. The PTB profile studied in this paper spans from the top part of the skeletal grainstone to the grayish micritic limestone.

2.2 Lithology, biota, microbialites, and biostratigraphy

The Xiushui profile was measured, examined in detail, and sampled at small intervals of 0.2 to 0.4 m. All rock samples were thin sectioned. Powder samples for carbon isotopic analysis were taken from the rock sample where thin section was made from and studied to evaluate the influence of diagenesis.

During fieldwork, the profile was divided into 40 subbeds (Figure 1). Based on examination of the thin sections, the 40 subbeds were grouped into 10 beds according to lithology.

The basal Bed 1 (= Subbed 1) (>5 m) is a grayish, massive spar-cemented skeletal grainstone. The skeletal grains include foraminifers, echinoderms, fusulinids (Figure 2a), and calcareous algae. The fusulinids include *Palaeofusulina* and *Nankinella*. The foraminifers include *Colaniella* (Figure 2b), *Climacammina*, *Glomospira*, *Pseudog-*

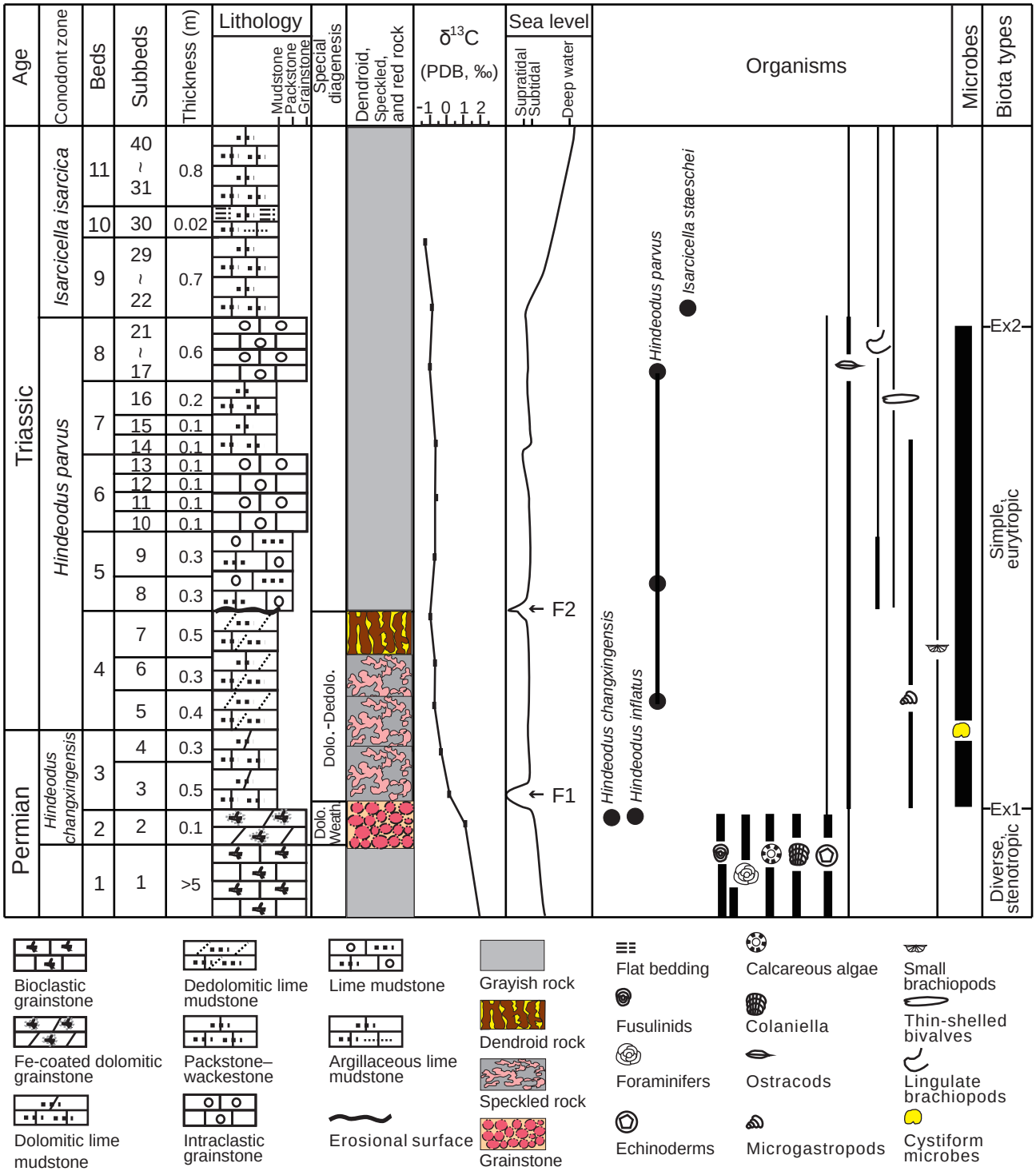

Figure 1 Lithology, conodonts, carbon isotopic composition, sea-level changes, biota, speckled rock, and dendroid rock in the Permian−Triassic boundary (PTB) section in Xiushui, Jiangxi Province, South China. Ex1 = the first episode of the mass extinction; Ex2 = the second episode of the mass extinction; F1 = the first large sea-level fall; F2 = the second substantial sea-level fall.

landulina, *Lunucammina*, *Hemigordius*, *Pachyphloia*, and *Cribrogenerina*. The calcareous algae include *Gymnocodium*, *Permocalculus*, and *Pseudovermiporella*.

Bed 2 (= Subbed 2) is a 0.1- to 0.2-m-thick reddish spar-cemented grainstone (Figure 3a). Though this bed is not thick, it occurs in all nearby measured sections in this area. Examination of thin sections shows that the skeletal grains are rounded or sub-rounded (Figure 2c), and are internally dolomitic (Figure 3b: “Dol”). The dolomite rhombi in the skeletal grains are generally subhedral to eu-

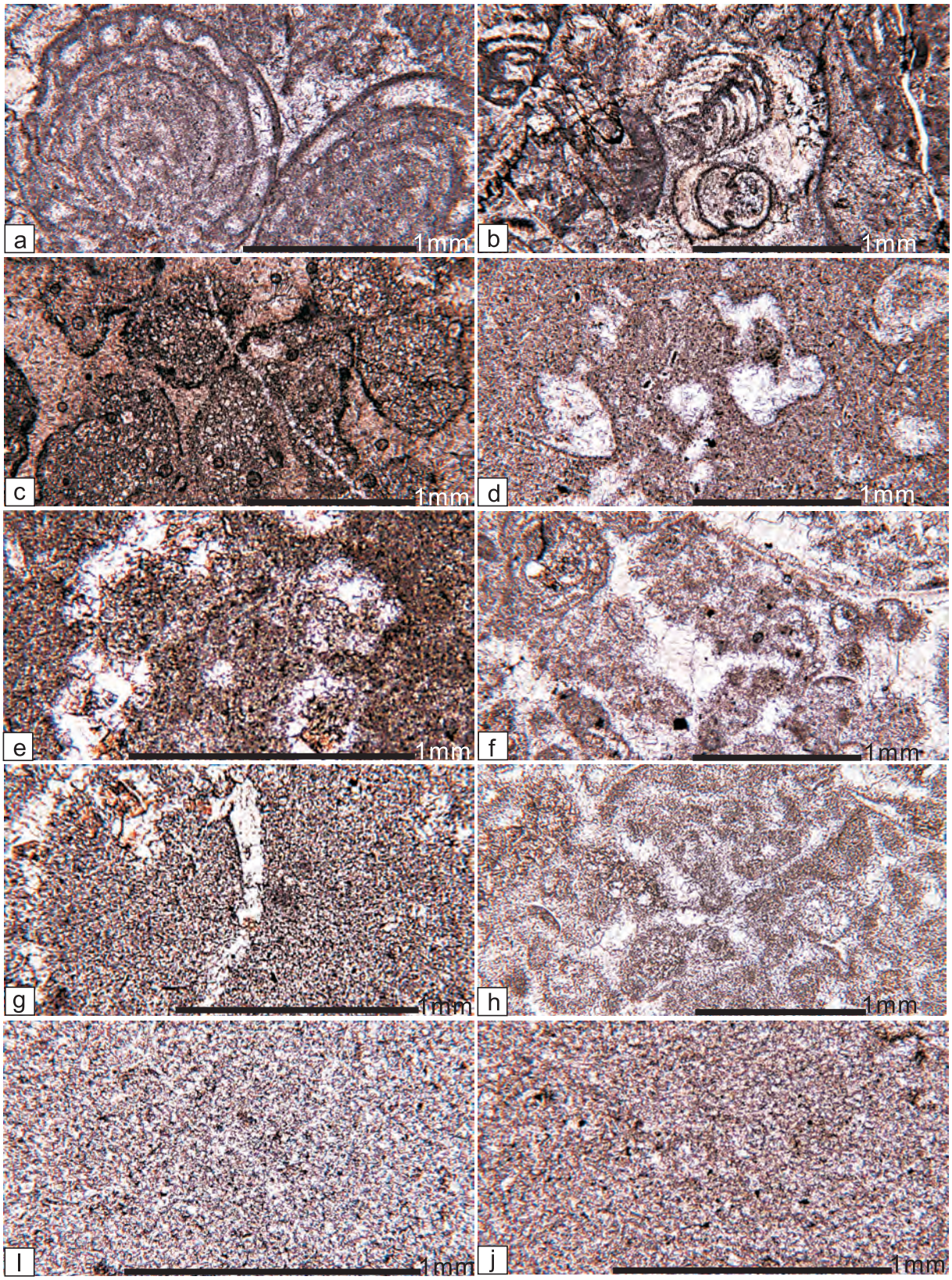

Figure 2 Microphotographs of thin sections showing the lithology and fossils, under plane-polarized light. a−Skeletal grainstone with fusulinid fossils, from Bed 1; b−Skeletal grainstone with large foraminifer *Colaniella*, from Bed 1; c−Skeletal grainstone composed of spar-cemented rounded skeletal grains with Fe-coating, from Bed 2; d−Lime mudstone, from Bed 3 (Subbed 3); e−Packstone, from Bed 3 (Subbed 4); f−Grainstone, from Bed 6 (Subbed 12); g−Lime mudstone, from Bed 7 (Subbed 15); h−Grainstone, from Bed 8 (Subbed 20); i−Lime mudstone, from Bed 9 (Subbed 26); j−Lime mudstone, from Bed 11 (Subbed 40).

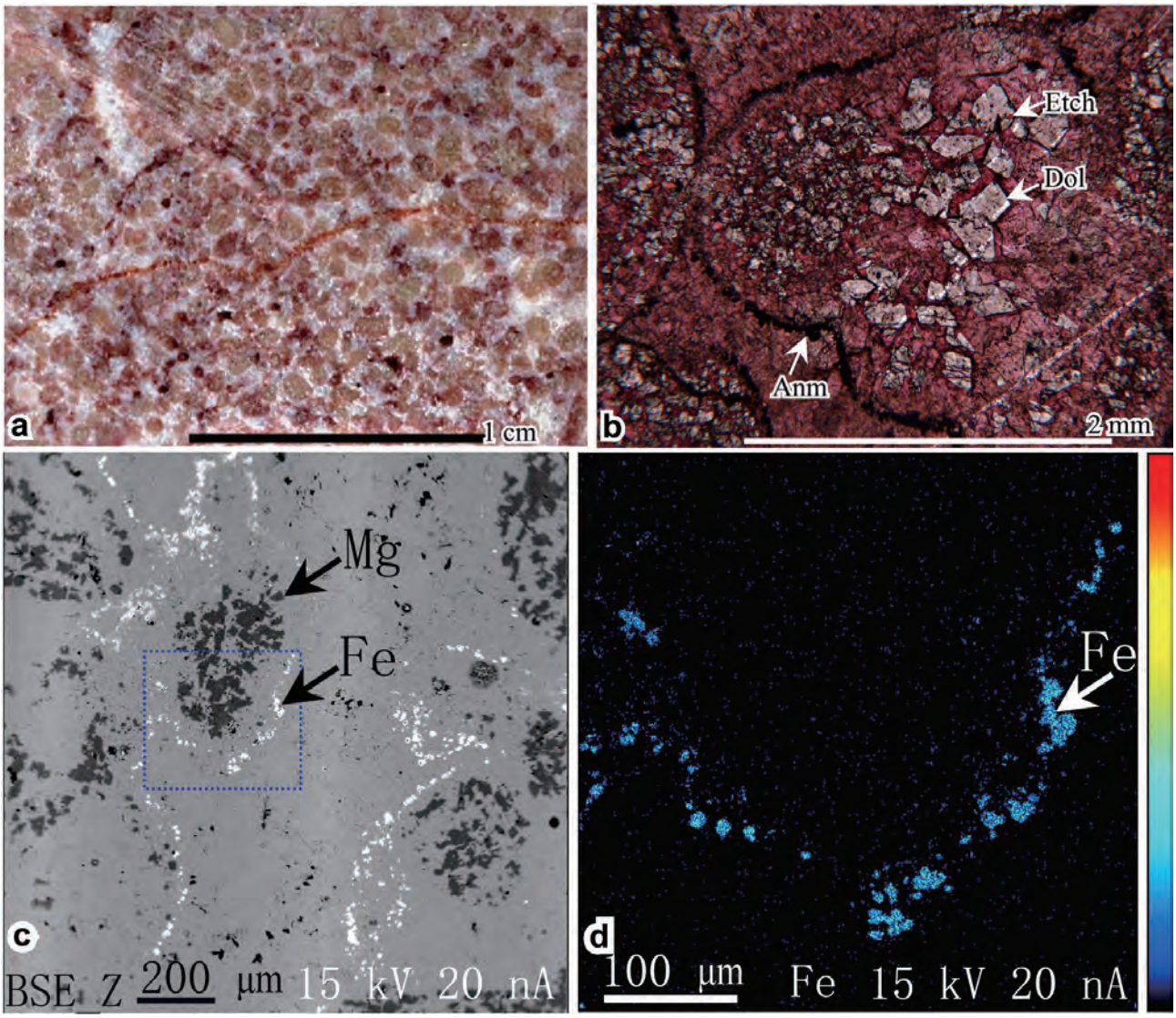

Figure 3 Microphotographs showing the fabric and composition of the reddish grainstone of Bed 2. a−Scanning picture of a slab; b−Microphotograph of a thin section, alizarin red stained, under plane-polarized light; c−Back-scattered electron (BSE) image of an area of the thin section; d−Enlargement of the blue marked square of c. The white dots in c and blue dots in d are the distribution of the Fe element. The dark dots of c are the distribution of the Mg element. Dol = dolomite; Etch = etched; Anm = anhedral mineral.

hedral, finely crystalline. They are similar in size in some grains, but are coarser in inner parts in other grains. Staining with alizarin red solution reveals that many dolomite rhombi had been etched (Figure 3b: "Etch"), and the solution pores had been filled by calcites. All grains have a thin coating layer composed of anhedral minerals (Figure 3b: "Anm"). Microprobe analysis reveals that the anhedral mineral is ferrous (Figure 3c, 3d: "Fe") in composition. Small brownish mineral grains in thin sections under polarized light or orthogonal light is limonite. Radio-axial calcite cements perpendicularly occur on the limonite layer. The second generation cement was larger blocky calcites. Though most grains have been dolomitized and lack original structure of the grains, some remain structure of *Colaniella*. Thus this bed is inferred to have the same skeletal composition as Bed 1.

Bed 3 (= Subbeds 3 and 4) and lower Bed 4 (Subbeds 5 to 6) is a 1.5-m-thick medium-bedded speckled limestone. On outcrops, it is composed of irregular reddish spots (Figure 4a, 4b: "Red") embedded in grayish areas (Figure 4a, 4b: "Gra"). The grayish areas accounts for about 45% of the rock, and is mainly a micritic limestone (Figure 2d), but locally are wackestone (Figure 2e) and packstone. The reddish areas accounts for about 55% of the rock, and is composed of dolomitic limestone. This study reveals that the reddish areas are resultant from the transformation

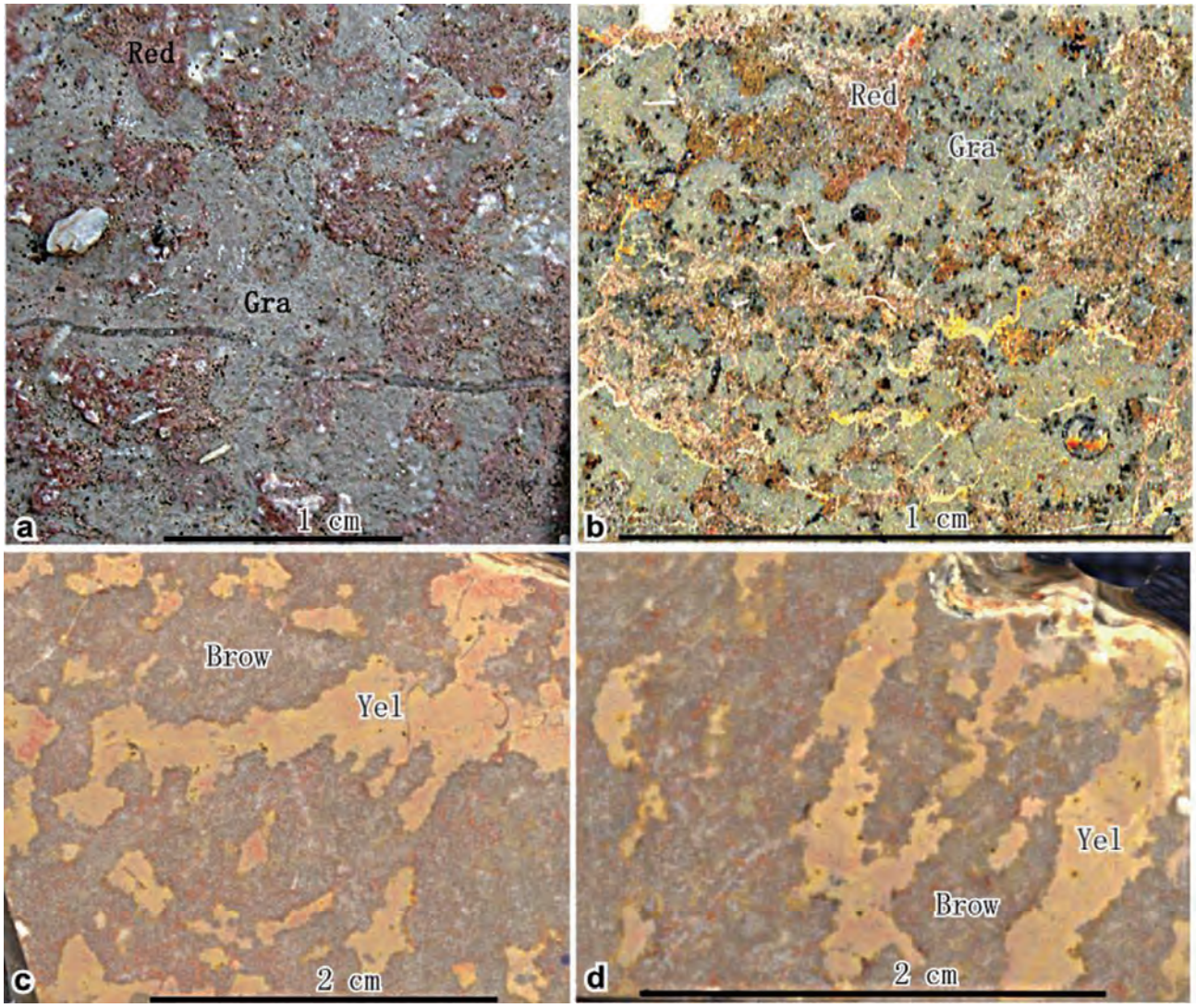

Figure 4 Photos showing the macroscopic appearance of the speckled rock (a, b) of Bed 3 and low Bed 4 and the dendroid rock (c, d) of the upper Bed 4. a−Outcrops; b to d−Slabs. Red = the reddish spots; Gra = the gray areas; Brow = the brownish areas; Yel = the yellowish areas.

of previous packstone, wackestone, and locally the same micritic limestone as the grayish areas. Cystiform microbial fossils, which have been assigned to the colonial cyanobacterium *Microcystis* (Wu *et al.*, 2014), ostracods, small gastropods, and small bivalves have been found from Bed 3 (= Subbeds 3 and 4) and lower Bed 4, and all have low diversity. The fusulinids, *Colaniella*, and calcareous algae that once occurred in the underlying beds are all absent from these beds. There seems to be more abundant fossils in the reddish dolomitic limestone areas than in the grayish areas, and they seem to have been more severely destroyed by diagenesis than those in the grayish areas.

The upper Bed 4 (Subbed 7) is a 0.5-m-thick dendroid rock. On outcrops, it is composed of brownish dendroid areas (Figure 4c, 4d: "Brow") embedded in irregular yellowish areas (Figure 4c, 4d: "Yel"). The brownish dendroid areas accounts for about 70% of the rock, and is mainly composed of coarser calcites; the yellowish areas accounts for about 30%, and is mainly composed of micritic limestone. This study reveals that the brownish dendroid areas are formed from previous packstone, wackestone, and the same micritic limestone as the yellowish areas. Previously, these areas contain small fossils, especially microbial fossils (probably belonging to *Microcystis*). Currently the fossils have been changed to patches of large euhedral calcites and anhedral calcite cements between them. The micritic matrix between the previous small fossils has been changed to small anhedral calcites due to recrystallization. The top surface of Bed 4 is wavy, and probably represents an ancient erosional surface.

Bed 5 (= Subbeds 8 to 9) is a 0.6-m-thick grayish, medium-bedded packstone. It contains ostracods, some small lingulate brachiopods, some thin-shelled bivalves (probably belonging to Pinnidae), and some *Microcystis* fossils (Wu *et al.*, 2014).

Bed 6 (= Subbeds 10 to 13) is a 0.4-m-thick grayish, medium-bedded spar-cemented bioclastic grainstone (Figure 2f). It contains some small brachiopods, small bivalves, thin-shelled bivalves, ostracods, small gastropods, and some *Microcystis* fossils.

Bed 7 (= Subbeds 14 to 16) is a 0.4-m-thick grayish, medium-bedded lime mudstone. It contains some small brachiopods (Figure 2g), small bivalves, thin-shelled bivalves, ostracods, and some unknown microbial fossils.

Bed 8 (= Subbeds 17 to 21) is a 0.6-m-thick grayish, medium-bedded spar-cemented grainstone (Figure 2h), containing some ostracods, thin-shelled bivalves, some small lingulate brachiopods, some thin-stemmed crinoids, and some *Microcystis* fossils. This bed is characteristically thin-bedded, obviously different from the overlying and underlying medium-bedded beds. Its contact surfaces with the overlying and the underlying beds are conformable.

Bed 9 (= Subbeds 22 to 29) is a 0.7-m-thick grayish, medium-bedded lime mudstone (Figure 2i), containing some ostracods and some thin-shelled bivalves.

Bed 10 (= Subbed 30) is a 0.02-m-thick dark-colored argillaceous lime mudstone, with flat laminated bedding, which probably indicates stagnant sedimentary environments.

Bed 11 (= Subbeds 31 to 40) is a 0.8-m-thick medium-bedded lime mudstone (Figure 2j). It contains sparse small ostracods, thin-shelled bivalves, and small lingulate brachiopods. The above stratum is the same medium-bedded lime mudstone.

3 Conodont biostratigraphy

The conodont zones of the P−T transition of Meishan section, the GSSP of the PTB, is used as a standard of biostratigraphic division. As seen in Table 1, the P−T transition of Meishan section has been divided into 8 beds or subbeds in ascending order (Yin *et al.*, 2001): 24e, 25, 26, 27a, 27b, 27c, 27d, and 28. The eight beds or subbeds are assigned to 4 conodont zones (Yin *et al.*, 2001): 24e to *Clarkina yini* Zone, 25 and 26 to *C. meishanensis* Zone, 27a and 27b to *Hindeodus typicalis* Zone, 27c and 27d to *H. parvus* Zone, and 28 to *Isarcicella isarcica* Zone. After restudying and revising some of the conodonts, Wu (2005a) made a small revision on Yin *et al.* (2001)′s division: 24e and 25 to *C. yini* Zone, 26 to *C. meishanensis* Zone, 27a and 27b to *Hindeodus changxingensis* Zone, 27c and 27d to *H. parvus* Zone, and 28 to *I. staeschei* Zone. The *C. yini* Zone is distinguished by the presence of *C. yini*, the *C. meishanensis* Zone by *C. meishanensis*, *H. changxingensis* Zone by *H. changxingensis*, the *H. parvus* Zone by *H. parvus*, and the *I. staeschei* Zone by *I. staeschei*. Since the *Hindeodus typicalis* identified by different researchers are not always the same, but it is not the case for *Hindeodus changxingensis*, the revised scheme by Wu (2005a) has some advantage.

The Xiushui profile yields abundant conodont fossils. The conodont fossils are dominated by *Hindeodus* components (Figure 5). *Hindeodus changxingensis* (Figure 5a), the critical component of the *H. changxingensis* Zone of the Meishan section (Wu, 2005a, 2005b) has been found in Bed 2. So, Bed 2 belongs to the *H. changxingensis* Zone. Bed 3 lacks *Hindeodus parvus* and has been assigned to the same conodont zone as Bed 2. *Hindeodus parvus* (Figure 5b), the key component of the *H. parvus* zone, does not

Table 1 Conodont zones of the Meishan section

Bed	Yin *et al.* (2001)	Wu (2005a)
28	*Isarcicella isarcica* Zone	*Isarcicella staeschei* Zone
27d	*Hindeodus parvus* Zone	*Hindeodus parvus* Zone
27c		
27b	*Hindeodus typicalis* Zone	*Hindeodus changxingensis* Zone
27a		
26	*Clarkina meishanensis* Zone	*Clarkina meishanensis* Zone
25		*Clarkina yini* Zone
24e	*Clarkina yini* Zone	

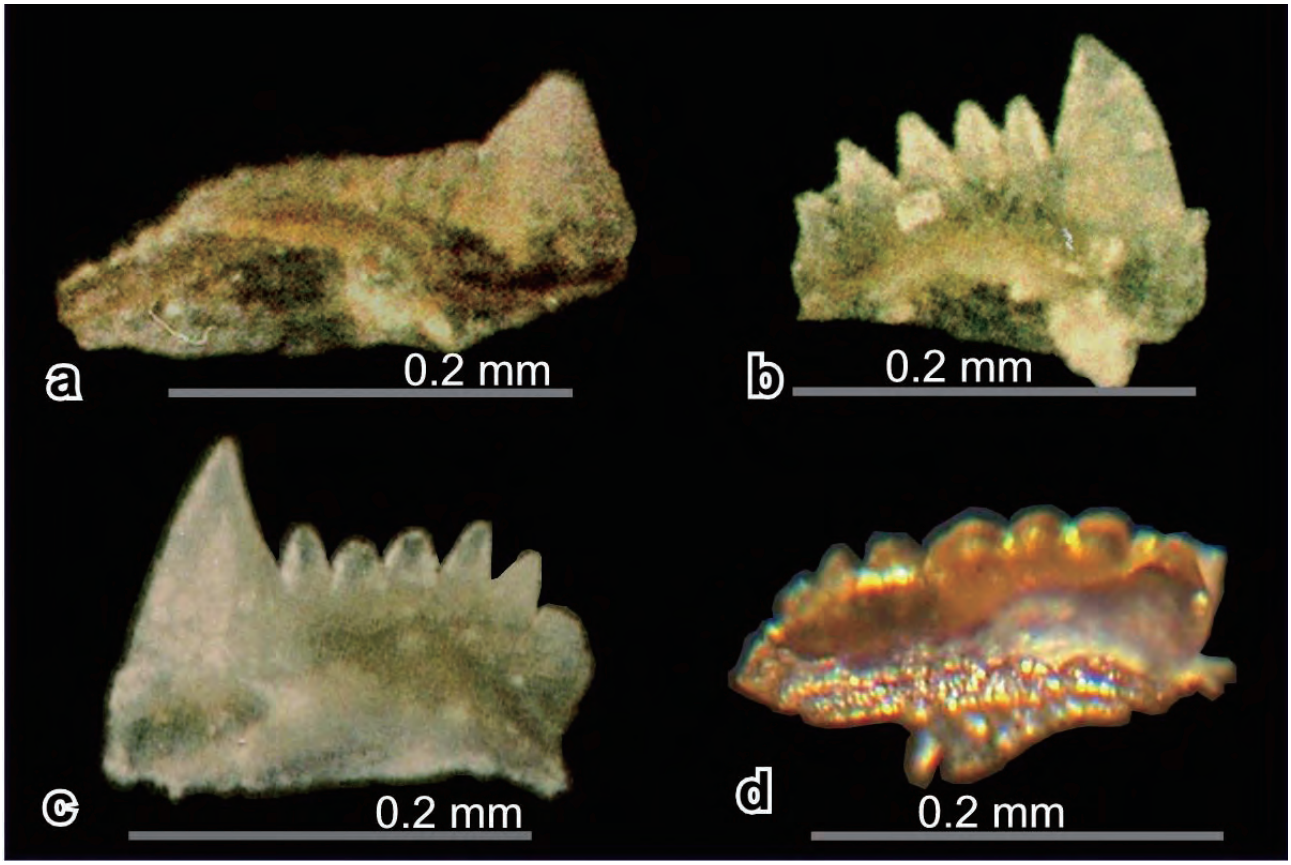

Figure 5 Key conodonts from the Permian−Triassic boundary section in Xiushui, Jiangxi Province, South China. a−*Hindeodus changxingensis*, from Bed 2; b−*Hindeodus parvus*, from the base of Bed 4 (Subbed 5); c−*Hindeodus parvus*, from the base of Bed 8 (Subbed 17); d−*Isarcicella staeschei*, from the base of Bed 9 (Subbed 22).

occur till basal Bed 4. So the P−T boundary lies at the base of Bed 4. Bed 8 (Subbed 17) still yields typical *H. parvus* (Figure 5c). So, Bed 4 through Bed 8 are assigned to *H. parvus* Zone. *Isarcicella staeschei* (Figure 5d) does not occur till basal Bed 9. Thus the base of Bed 9 is regarded as the base of *Isarcicella staeschei* Zone (Wu, 2005a).

4 Biotic evolution and mass extinction

The biota in beds 1 and 2 is diverse, dominated by stenotropic organisms including fusulinids, calcareous algae, and large foraminifer *Colaniella*. Foraminifer *Colaniella* and fusulinid *Palaeofusulina* are typical pre-extinction Permian organisms (Wu *et al.*, 2007a). Their presence in Bed 2 (Figure 2a, 2b) indicates that the biota in Bed 2 is of pre-extinction.

All the stenotropic organisms of Bed 2, especially the symbolic foraminifer *Colaniella* and fusulinid *Palaeofusulina*, suddenly disappeared at the end of Bed 2. The extinction of the typical Permian stenotropic organisms has been regarded as the first episode of the end-Permian mass extinction (Yin *et al.*, 2007; Wu *et al.*, 2007a). Thus the main extinction episode in this area happened at the end of Bed 2, before the beginning of the *Hindeodus changxingensis* zone.

The biota in Bed 3 through Bed 8 is composed of abundant ostracods, cyanobacterial *Microcystis*, microgastropods, small brachiopods, thin-shelled bivalves, and echinoderms. *Microcystis* are generally regarded as eurytropic type (Ezaki *et al.*, 2003, 2008; Wang *et al.*, 2005b; Wu *et al.*, 2007a, 2007b), and can survive or flourish in very extreme environments intolerable to other organisms. Ostracods, microgastropods, and thin-shelled bivalves have been reported to occur in the PTB sections in Guizhou and other places, and interpreted to be eurytropic components tolerant of the unusual environments following the extinction. So, the post-extinction biota in the Xiushui section was dominated by eurytropic types.

The biota in Bed 9 through Bed 11 is composed of very sparse ostracods, thin-shelled bivalves, and small lingulate brachiopods. The abundant microbes and microgastropods, as well as the echinoderms that once bloomed in Beds 3 to

8, are all absent from Beds 9 to 11. Photoautotrophic microbes, especially cyanobacterial *Microcystis*, cannot live in deep waters. The microbes of the P−T transition were generally regarded as dominated by cyanobacteria (Wang *et al.*, 2005b). Their absence from Beds 9 to 11 might reflect the water depth had become too deep. The disappearance of microgastropods, cyanobacterial *Microcystis* and echinoderms before the deposition of Bed 9 may represent another small episode of the mass extinction (Wu *et al.*, 2007a). The biotic evolution during the latest Permian and the earliest Triassic in this area includes three stages. The first is the diverse biota dominated by stenotropic organisms in Beds 1 and 2. The second is the simple biota dominated by eurytropic organisms in the Beds 3 to 8. The third is the very simple biota consisting of sparse ostracods, a few thin-shelled bivalves, and possibly a few lingulate brachiopods in Beds 9 to 11.

The first biota lived in a normal open carbonate platform condition favorable to most organisms. The second biota dwelled in a restricted shallow marine environment. The third biota is possibly related to a deep-water environment, which was probably low-oxygenated in some periods, as indicated by the dark deposits of Subbed 30.

5 Sedimentary environmental change and sea-level fall

The spar-cemented grainstone of Bed 1 represents shallow marine, generally skeletal bank environments. The presence of fusulinids and calcareous algae indicates warm, normal shallow marine conditions.

Bed 2 is also a grainstone, and the skeletal composition of grains is similar to that of Bed 1. Thus, the sedimentary environment of Bed 2 is similar to that of Bed 1. The grains in Bed 2, however, are mostly rounded, indicating stronger wavy action than that of Bed 1. The change from the angular skeletal grains of Bed 1 to the rounded grains of Bed 2 reflects a decrease in water depth and increase in wave action.

The reddish color of Bed 2 reminds us of red deposits common in many geological times and related to subaerial weathering. The limonite coating on the skeletal grains was originated from weathering under subaerial conditions. The lift of the sediments and their entering into subaerial environments need a sea-level fall before the grains were cemented. The dolomitization of the grains might be related to the impact of evaporate concentrated seawater in supratidal environments. The fabric features of the dolomite rhombi in the grains, generally small, finely crystalline, subhedral to euhedral, support this interpretation. The formation of the etched pores in the relict dolomite rhombi might be related to affection of meteoric freshwater under a subaerial condition. Thus the reddish grainstone recorded a substantial sea-level fall event, which happened after the deposition of Bed 2.

The deposition of Beds 3 and 4 needs a sea-level rise to form the accommodating space. Thus a sea-level rise is suggested to have happened from the beginning of the deposition of Bed 3. Since the lithology of Beds 3 and 4 is dominated by micrites and their biota lacks tidal types, the sedimentary environments of Beds 3 and 4 were more than 20 m in depth, and the sea-level rise had a magnitude of more than 20 m. The occurrence of cyanobacterial *Microcystis* fossils in Beds 3 and 4 might reflect that the sedimentary environments of these beds were very unusual, such as with low dissolved oxygen (Kershaw *et al.*, 1999, 2002; Ezaki *et al.*, 2003, 2008; Wang *et al.*, 2005b; Wu *et al.*, 2014).

The lithology of Beds 3 and 4 is characterized by the speckled and dendroid microscopic appearance. The same features are present in the speckled and dendroid microbialites in the PTB section at Laolongdong, Chongqing, China (Jiang and Wu, 2013). Jiang and Wu (2013) found that diagenesis has played an important role in the formation of the speckled and dendroid appearance of the microbialites of the Laolongdong section. This study reveals that diagenesis has played the same role in the formation of the speckled and dendroid appearance of Beds 3 and 4 of Xiushui section.

Both of Beds 3 and 4 have suffered dolomitization, as indicated by the complete or incomplete dirty-cored dolomite rhombi. There is much more dirty-cored dolomite rhombi in Bed 4 than in Bed 3. This leads one to infer that the concentrated brine of dolomitization migrated from Bed 4 to Bed 3, in a downward direction. The downward migration of dolomitizing fluid suggests a supratidal evaporate model of dolomitization (Illing *et al.*, 1965; Hsü and Siegenthaler, 1969). Such a model needs a sea-level fall to let the sediments enter into a supratidal environment. Thus we infer that the sediments of Beds 3 and 4 once entered into supratidal environments, where they became dolomitized.

A dedolomitization event had altered Bed 4, having changed most euhedral dirty-cored dolomite rhombi to euhedral dirty-cored calcite rhombi. Observation shows the affection of the dedolomitization on Bed 3 is much less than on Bed 4. This suggests that the migration of the dedolomitization fluid migrated in a downward direction. Less

dedolomitization fluid had reached Bed 3, especially its lower part, and less calcite rhombi formed in Bed 3.

Many hypotheses have been proposed to interpret the mechanisms of dedolomitization. Based on experimental results, deGroot (1967) proposed that dedolomitization is a process generally occurring in a subaerial environment with a lower Pco_2, lower temperature (<50ºC), and high water-rock ratio. His model is supported by many case studies (Arenas *et al.*, 1999; Zeeh *et al.*, 2000; Rameil, 2008). Kenny (1992) reported a dedolomitic rock in the several meters of dolostone below the Devonian disconformity, and believed that the dedolomitization was caused by the action of the meteoric water. The distribution of the calcite rhombi in Beds 3 and 4 of Xiushui section is consistent with a meteoric water model.

Since Bed 5 does not contain dolomite or dedolomitized rhombi, the dolomitization and dedolomitization have affected Beds 4 and 3. It is reasonable to infer the sediments of Beds 4 and 3 once entered into supratidal environments due to a sea-level fall and uplift of the basin. The top of Bed 4 is wavy, and seems to be an erosional surface. Since laterally tracing the outcrops is impossible, we cannot go further in determining the nature of the top surface. If the top surface is really an erosional surface, it indicates that the sea-level fall has a relatively big magnitude and relatively long duration. If it is not an erosional surface, it does not deny the presence of a relative sea-level fall.

The deposition of Bed 5 (Subbeds 8 and 9) needs a sea-level rise to form accommodating space. Bed 5 is thin (0.6 m) and is a packstone. The sparry cement in the skeletal grainstone of Bed 6 indicates that the sedimentary environments of the Bed 6 had a water depth smaller than that of Bed 5, which was probably caused by the accumulation of sediments. So, Beds 5 and 6 constitute a shoaling-up cycle.

The lime mudstone of Bed 7 represents deeper water than Bed 6, which needs a slight rise of the sea level. The spar-cemented grainstone in Bed 8 represents shallower water than Bed 7. The biota in Bed 8 is similar to that of Bed 7. But, the water depth decreased, which means a small sea-level fall or the result of sediment accumulation. Nevertheless, Beds 7 and 8 constitute another small shoaling-up cycle. .

The lime mudstone of Bed 9 represents deeper water than Bed 8, which means a slight rise in the sea level. The flat beddings in Bed 10 indicate a stagnant condition and water depth below the wave base. Absence of benthic fossils from Beds 9 and 11 probably reflects some extreme marine conditions, such as a low-oxygenated environment, which could be the result of sea-level rise, as proposed by Wignall and Hallam (1992, 1996).

Bed 11 and the above many meters are the same lime mudstone containing very sparse fossils, representing relatively deep water. So Beds 9 to 11, and some of the above thickness make up a deepening-up cycle.

In summary, the PTB section in Xiushui has recorded two substantial sea-level falls, a following period of slow rise, and the later quick rise. The stagnant and probably anoxic water caused by the quick rise was inadaptable to all organisms.

6 Discussion

6.1 Sea-level fall in the P−T transition

How did the sea level changed during the P−T transition? The dispute has continued for many years since Wignall and Hallam (1992, 1996) proposed that there was no sea-level drop but sea-level rise during the period from the latest Permian to the earliest Triassic, and that it was the oceanic anoxia caused by the continuing sea-level rise that triggered the mass extinction. But, in the last decade, more and more studies are presenting opposite evidences. Wu *et al.* (2003) made a systematic study on the sedimentologic and diagenetic records of a sea-level fall in the latest Permian on the Changhsingian reef in Ziyun, Guizhou Province, China, and determined this sea level has an amplitude about 89.3 m. They also determined the amplitude of a coeval sea level in Hubei province, South China to be about 88.9 m, and suspected that it is a eustatic sea-level fall. Wu *et al.* (2006a, 2006b) reported evidences for an end-Permian sea-level fall in Xiushui, Jiangxi Province, and at Laolongdong, Chongqing. Ezaki *et al.* (2003) noticed an erosional surface in a PTB section in Langpai area, Luodian, Guizhou Province. Zhang *et al.* (2006) proposed that a large sea-level fall occurred in the latest Permian in Dongpan, Guangxi Province. Farabegoli *et al.* (2007) noticed two unconformity surfaces in the latest Permian of the Bulla and Tesero sections in Southern Alps (Italy). Heydari *et al.* (2003) proposed that there is an end-Permian sea-level fall in the PTB section in Abadeh, Iran. Ezaki *et al.* (2008) reported the presence of an unconformable surface as the bottom of the P−T boundary thrombolites. Collin *et al.* (2009) reported pendent and meniscus cements in the Great Bank of Guizhou (GBG), South China, proving a lowstand. Wu *et al.* (2010) made a detailed study on the sedimentologic evidences for an end-Permian sea-level fall at the top of the Changhsingian reef

in Ziyun. Since evidences for an end-Permian sea-level fall have been found in so many places over the world, Wu *et al.* (2010) proposed that the end-Permian sea-level fall might be eustatic. Kershaw *et al.* (2011) found a major erosion surface in the PTB sequence, near Antalya, Turkey, and interpreted it as being the Late Permian lowstand, as well as several small-scale erosions in the deposits above the mass extinction horizon. Wang *et al.* (2012) found a sea-level fall in the PTB section at Dawen of Luodian, Guizhou Province, South China, and believed they were of a global scale. Liu *et al.* (2014) reported evidences of a big sea-level fall at the horizon of the first and main mass extinction episode.

6.2 Mass extinction pattern

This study reveals that the mass extinction consists of a main episode happening at the horizon about 0.8 m below the P−T boundary, and a small second episode at the end of the *Hindeodus parvus* zone. This conclusion is in accordance with the case in Bükk Mountain, Northern Hungary (Haas *et al.*, 2007), where a biotic crisis began from about 1 m below the bottom of the *H. parvus* zone. The mass extinction in Meishan section, the GSSP of the P−T boundary, is believed to include a main episode at 251.4 Ma and the decline of the remaining taxa in the following 1 Ma (Jin *et al.*, 2000). Yin *et al.* (2007) believed the PTB mass extinction consists of three episodes, with the first one at the bottom of Bed 24e, about 0.2 m below the P−T boundary. Yang *et al.* (1991) studied 14 PTB sections in South China, and found that an obvious extinction "line" is present at meters to tens of centimeters below the P−T boundary. Wu *et al.* (2007a) studied two reef-related PTB sections in Guizhou Province, China, and found that the extinction of reef ecosystems at the end of the Permian include two steps: the first is the extinction of the stenotropic organisms at the horizon 1.7 to 2.4 m below the P−T boundary, and the second is the extinction of most eurytropic organisms at the bottom of *H. parvus* zone. Noé (1987) studied the PTB section in Tesero, Italy, and found that 72% of marine species including fusulinids became extinct at 2.2 m below the P−T boundary, which was regarded as the first extinction episode by the present authors, and most eurytropic species became extinct at the bottom of the *H. parvus* zone, which was considered as the second extinction episode by us. Wignall and Newton (2003) studied the PTB section in Ursula Creek, British Columbia, Canada, and found that the first extinction event, the extinction of radiolarians, happened at 1.6 m below the P−T boundary, and the second extinction event, the extinction of siliceous sponges, happened at 0.8 m below the P−T boundary. Twitchett *et al.* (2001) found that in Jameson Land, eastern Greenland, the first extinction happened at several meters below the P−T boundary. All previous researches revealed that the first mass extinction episode happened at some distance below the P−T boundary. This study supports their results, and determines that it occurred at the base of the conodont *Hindeodus changxingensis* zone. This conodont zone was defined by Wu (2005a), and occupies the duration between the *Clarkina meishanensis* zone and *Hindeodus parvus* zone. So, the main episode of the mass extinction happened before the beginning of the Mesozoic.

6.3 Relationship between mass extinction and sea-level fall

As indicated by the coating on the skeletal grains of the grainstone, a substantial sea-level fall occurred after the deposition of Bed 2. Interestingly, the first drastic biotic change occurred at about the same time, after the deposition of Bed 2. Is it an accidental coincidence or it reflects a causal relationship? Two reasons made us prefer to the latter.

A causal relationship between a sea-level fall and a mass extinction is possible. A substantial sea-level fall can be caused by (1) changes in the total volume of oceanic water on the earth because of drastic global climatic changes, and (2) changes in the total volume of the oceanic crust because of changes in the expanding speed of oceanic ridges. Based on the ecological type of the extinct taxa, Wu (2005a) has proposed the possibility of a drastic climatic cooling as the triggering mechanism of the end-Permian mass extinction. A drastic cooling event can greatly reduce the total volume of oceanic water through ice sheet increase, and cause a substantial sea-level fall. A drastic climatic cooling event can killed all stenotrophic thermophilous organisms, such as reef-building calcareous sponges and corals, causing mass extinction in the marine and land biosphere. Thus, a substantial eustatic sea-level fall can occur at about the same time as a mass extinction happens, both as the result of a drastic climatic cooling event. Sun *et al.* (2012) reported a conodont oxygen isotope evidence for P−T transition warming. However, their warming event occurred after the mass extinction, and cannot be considered as the cause of the extinction. Secondly, not only in Xiushui, the sea-level fall occur at the same time as the first episode of the mass extinction, but also in many other places. Wu *et al.* (2007a) have found that the mass extinction of reef ecosystems in the

P−T transition in Ziyun, Guizhou Province, South China happened in two steps. The first is the sudden disappearance of all stenotropic organisms including calcisponges and fusulinids in the *Clarkina yini* Zone, and the second is the disappearance of most eurytropic organisms including microgastropods and algal mats at the beginning of the *Hindeodus parvus* Zone. Yin *et al.* (2007) found that the prelude of the end-Permian mass extinction in Meishan section commenced during the time between Beds 24e and 25 and coincided with the end-Permian regression. The current study reveals that the first mass extinction episode in Xiushui section was coeval with the main end-Permian sea-level fall, both at the base of *Hindeodus changxingensis* zone. Such coevality may indicate that both of them have a common triggering mechanism, which probably is a drastic climatic cooling.

7 Conclusions

This study has reached the following points:

1) A substantial sea-level fall occurred in beginning of *Hindeodus changxingensis* Zone. It caused the skeletal grain deposits to be exposed to a subaerial environment, as indicated by the reddish Fe-coating on the skeletal grains.

2) The first and main episode of the mass extinction occurred in the beginning of *Hindeodus changxingensis* Zone, at about the same time as the substantial sea-level fall occurred, and is characterized by the sudden disappearance of all stenotropic warm-water organisms such as large foraminifers and dasycladacians.

3) The coevality of the sea-level fall and the main mass extinction episode is not accidental but causal. Probably a drastic climatic cooling has caused both of them.

Acknowledgements

This work was supported by the National Natural Scientific Foundation of China (Nos. 40472015 and 40802001), the State Key Laboratory of Modern Paleontology and Stratigraphy (No. 083113), the postdoctoral funds of China (No. 20070420523), and the State Key Laboratory of Geological Processes and Mineral Resources (GPMR2007−01).

References

Adachi, N., Ezaki, Y., Liu, J. B., 2004. The fabrics and origins of peloids immediately after the end-Permian extinction, Guizhou Province, South China. Sedimentary Geology, 164(1−2): 161−178.

Algeo, T. J., Hannigan, R., Rowe, H., Brookfield, M., Baud, A., Krystyn, L., Ellwood, B. B., 2007. Sequencing events across the Permian−Triassic boundary, Guryul Ravine (Kashmir, India). Palaeogeography, Palaeoclimatology, Palaeoecology, 252(1−2): 328−346.

Arenas, C., Alonso Zarza, A. M., Pardo, G., 1999. Dedolomitization and other early diagenetic processes in Miocene lacustrine deposits, Ebro Basin (Spain). Sedimentary Geology, 125(1−2): 23−45.

Benton, M. J., Tverdokhlebov, V. P., Surkov, M. V., 2004. Ecosystem remodelling among vertebrates at the Permian−Triassic boundary in Russia. Nature, 432(7013): 97−100.

Cao, C. Q., Love, G. D., Hays, L. E., Wang, W., Shen, S. Z., Summons, R. E., 2009. Biogeochemical evidence for euxinic oceans and ecological disturbance presaging the end-Permian mass extinction event. Earth and Planetary Science Letters, 281(3−4): 188−201.

Chen, Z. Q., Kaiho, K., George, A. D., Tong, J. N., 2006. Survival brachiopod faunas of the end-Permian mass extinction from the southern Alps (Italy) and South China. Geological Magazine, 143(3): 301−327.

Collin, P. Y., Kershaw, S., Crasquin-Soleau, S., Feng, Q. L., 2009. Facies changes and diagenetic processes across the Permian−Triassic boundary event horizon, Great Bank of Guizhou, South China: A controversy of erosion and dissolution. Sedimentology, 56(3): 677−693.

deGroot, K., 1967. Experimental dedolomitization. Journal of Sedimentary Petrology, 37(4): 1216−1220.

Erwin, D. H., 1993. The Great Paleozoic Crisis: Life and Death in the Permian. New York: Columbia University Press, 1−327.

Ezaki, Y., Liu, J. B., Adachi, N., 2003. Earliest Triassic microbialite micro- to megastructures in the Huaying area of Sichuan Province, South China: Implications for the nature of oceanic conditions after the end-Permian extinction. Palaios, 18(4−5): 388−402.

Ezaki, Y., Liu, J. B., Nagano, T., Adachi, N., 2008. Geobiological aspects of the earliest Triassic microbialites along the southern periphery of the tropical Yangtze Platform: Initiation and cessation of a microbial regime. Palaios, 23(6): 356−369.

Farabegoli, E., Perri, M. C., Posenato, R., 2007. Environmental and biotic changes across the Permian−Triassic boundary in western Tethys: The Bulla parastratotype, Italy. Global and Planetary Change, 55(1−3): 109−135.

Feng, Q. L., He, W. H., Gu, S. Z., Meng, Y. Y., Jin, Y. X., Zhang, F., 2007. Radiolarian evolution during the latest Permian in South China. Global and Planetary Change, 55(1−3): 177−192.

Haas, J., Demény, A., Hips, K., Zajzon, N., Weiszburg, T. G., Sudar, M., Pálfy, J., 2007. Biotic and environmental changes in the Permian−Triassic boundary interval recorded on a western Tethyan ramp in the Bükk Mountains, Hungary. Global and Planetary Change, 55(1−3): 136−154.

He, W. H., 2005. Brachiopod miniaturization in the Permian−Trias-

sic life crisis in South China. Albertiana, 33(1): 37−38.

Heydari, E., Hassanzadeh, J., Wade, W. J., Ghazi, A. M., 2003. Permian−Triassic boundary interval in the Abadeh section of Iran with implications for mass extinction: Part 1 − Sedimentology. Palaeogeography, Palaeoclimatology, Palaeoecology, 193(3−4): 405−423.

Hsü, K. J., Siegenthaler, C., 1969. Preliminary experiments on hydrodynamic movement induced by evaporation and their bearing on the dolomite problem. Sedimentology, 12 (1−2): 11−25.

Illing, L. V., Wells, A. J., Taylor, J. C. M., 1965. Penecontemporary dolomite in the Persian Gulf. In: Pray, L. C., Murray, R. C., (eds). Dolomitization and Limestone Diagenesis. SEPM Special Publications, 13: 89−111.

Jiang, H. X., Wu, Y. S., 2007a. Origin of microbialite-like dendroid rocks in the Permian−Triassic boundary section in Xiushui, Jiangxi Province. Geological Review, 53(3): 323−328 (in Chinese with English abstract).

Jiang, H. X., Wu, Y. S., 2007b. Restudy of the microbialite from the Permian−Triassic boundary section, Chongqing. Acta Petrologica Sinica, 23(5): 1189−1196 (in Chinese with English abstract).

Jiang, H. X., Wu, Y. S., 2013. Diagenesis of the microbialites in the Permian−Triassic boundary section at Laolongdong, Chongqing, South China. Journal of Palaeogeography, 2(2): 183−191.

Jin, Y. G., Wang, Y., Wang, W., Shang, Q. H., Cao, C. Q., Erwin, D. H., 2000. Pattern of marine mass extinction near the Permian−Triassic boundary in South China. Science, 289(5478): 432−436.

Kenny, R., 1992. Origin of disconformity dedolomite in the Martin Formation (Late Devonian, Northern Arizona). Sedimentary Geology, 78(1−2): 137−146.

Kershaw, S., Zhang, T. S., Lan, G. Z., 1999. A ?microbiolite carbonate crust at the Permian−Triassic boundary in South China, and its palaeoenvironmental significance. Palaeogeography, Palaeoclimatology, Palaeoecology, 146(1−4): 1−18.

Kershaw, S., Guo, L., Swift, A., Fan, J. S., 2002. ?Microbialites in the Permian−Triassic boundary interval in central China: Structure, age and distribution. Facies, 47(1): 83−89.

Kershaw, S., Li, Y., Crasquin-Soleau, S., Feng, Q. L., Mu, X. N., Collin, P. Y., Reynolds, A., Guo, L., 2007. Earliest Triassic microbialites in the South China block and other areas: Controls on their growth and distribution. Facies, 53(3): 409−425.

Kershaw, S., Crasquin, S., Forel, M. B., Randon, C., Collin, P. Y., Kosun, E., Richoz, S., Baud, A., 2011. Earliest Triassic microbialites in Çürük Dag, southern Turkey: Composition, sequences and controls on formation. Sedimentology, 58(3): 739−755.

Kershaw, S., Crasquin, S., Li, Y., Collin, P. Y., Forel, M. B., Mu, X. N, Baud, A., Wang, Y., Xie, S., Maurer, F., Guo, L., 2012. Microbialites and global environmental change across the Permian−Triassic boundary: A synthesis. Geobiology, 10(1): 25−47.

Kozur, H. W., 2007. Biostratigraphy and event stratigraphy in Iran around the Permian−Triassic Boundary (PTB): Implications for the causes of the PTB biotic crisis. Global and Planetary Change, 55(1−3): 155−176.

Krystyn, L., Richoz, S., Baud, A., Twitchett, R. J., 2003. A unique Permian−Triassic boundary section from the Neotethyan Hawasina Basin, Central Oman Mountains. Palaeogeography, Palaeoclimatology, Palaeoecology, 191(3−4): 329−344.

Liu, L. J., Jiang, H. X., Wu, Y. S., Cai, C. F., 2014. Community replacement sequences and paleoenvironmental changes in reef areas of South China from Late Permian to Early Triassic exemplified by Panlongdong section in northeastern Sichuan Basin. Science China Earth Sciences, 57(5): 1093−1108.

Noé, S. U., 1987. Facies and paleogeography of the marine Upper Permian and of the Permian−Triassic boundary in the Southern Alps (Bellerophon Formation, Tesero Horizon). Facies, 16(1): 89−141.

Rameil, N., 2008. Early diagenetic dolomitization and dedolomitization of Late Jurassic and earliest Cretaceous platform carbonates: A case study from the Jura Mountains (NW Switzerland, E France). Sedimentary Geology, 212(1−4): 70−85.

Shen, S. Z., Cao, C. Q., Henderson, C. M., Wang, X. D., Shi, G. R., Wang, Y., Wang, W., 2006. End-Permian mass extinction pattern in the northern peri-Gondwanan region. Palaeoworld, 15(1): 3−30.

Shen, S. Z., Crowley, J. L., Wang, Y., Bowring, S. A., Erwin, D. H., Sadler, P. M., Cao, C. Q., Rothman, D. H., Henderson, C. M., Ramezani, J., Zhang, H., Shen, Y. A., Wang, X. D., Wang, W., Mu, L., Li, W. Z., Tang, Y. G., Liu, X. L., Liu, L. J., Zeng, Y., Jiang, Y. F., Jin, Y. G., 2011. Calibrating the end-Permian mass extinction. Science, 334(6061): 1367−1372.

Sun, Y. D., Joachimski, M. M., Wignall, P. B., Yan, C. B., Chen, Y. L., Jiang, H. S., Wang, L. N., Lai, X. L., 2012. Lethally hot temperatures during the Early Triassic greenhouse. Science, 338(6105): 366−370.

Twitchett, R. J., Looy, C. V., Morante, R., Visscher, H., Wignall, P. B., 2001. Rapid and synchronous collapse of marine and terrestrial ecosystems during the end-Permian biotic crisis. Geology, 29(4): 351−354.

Twitchett, R. J., Krystyn, L., Baud, A., Wheeley, J. R., Richoz, S., 2004. Rapid marine recovery after the end-Permian mass-extinction event in the absence of marine anoxia. Geology, 32(9): 805−808.

Wang, C. J., Liu, Y. M., Liu, H. X., Zhu, L., Shi, Q., 2005a. Geochemical significance of the relative enrichment of pristane and the negative excursion of $\delta^{13}C_{Pr}$ across the Permian−Triassic Boundary at Meishan, China. Chinese Science Bulletin, 50(19): 2213−2225.

Wang, Y. B., Tong, J. N., Wang, J. S., Zhou, X. G., 2005b. Calcimicrobialite after end-Permian mass extinction in South China and its palaeoenvironmental significance. Chinese Science Bulletin, 50(7): 665−671.

Wang, H. F., Liu, J. B., Ezaki, Y. 2012. Sea-level changes at the Dawen Permian−Triassic boundary section of Luodian, Guizhou Province, South China: A global correlation. Acta Scientiarum Naturalium Universitatis Pekinensis, 48(4): 589−602 (in Chinese with English abstract).

Weidlich, O., Kiessling, W., Flugel, E., 2003. Permian−Triassic

boundary interval as a model for forcing marine ecosystem collapse by long-term atmospheric oxygen drop. Geology, 31(11): 961−964.

Wignall, P. B., Hallam, A., 1992. Anoxia as a cause of the Permian/Triassic mass extinction: Facies evidence from northern Italy and the western United States. Palaeogeography, Palaeoclimatology, Palaeoecology, 93(1−2): 21−46.

Wignall, P. B., Hallam, A., 1996. Facies change and the end-Permian mass extinction in S.E. Sichuan, China. Palaios, 11(6): 587−596.

Wignall, P. B., Newton, R., 2003. Contrasting deep-water records from the Upper Permian and Lower Triassic of South Tibet and British Columbia: Evidence for a diachronous mass extinction. Palaios, 18 (2): 153−167.

Wu, Y. S., 2005a. Conodonts, Reef Evolution and Mass Extinction across the Permian−Triassic Boundary. Beijing: Geological Publishing House, 1−90.

Wu, Y. S., 2005b. Conodont evolution during Permian−Triassic transition in mid-low latitudes: A close-up view. Albertiana, 33(1): 93−94.

Wu, Y. S., Fan, J. S., Jin, Y. G., 2003. Emergence of the Late Permian Changhsingian reefs at the end of the Permian. Acta Geologica Sinica, 77(3): 289−296 (in Chinese with English abstract).

Wu, Y. S., Jiang, H. X., Liao, T. P., 2006a. Sea-level drops in the Permian−Triassic boundary section at Laolongdong, Chongqing, Sichuan Province. Acta Petrologica Sinica, 22(9): 2405−2412 (in Chinese with English abstract).

Wu, Y. S., Yang, W., Jiang, H. X., Fan, J. S., 2006b. Petrologic evidence for sea-level drop in the latest Permian in Jiangxi province, China and its meanings for the mass extinction. Acta Petrologica Sinica, 22(12): 3039−3046 (in Chinese with English abstract).

Wu, Y. S., Fan, J. S., Jiang, H. X., Yang, W., 2007a. Extinction pattern of reef ecosystems in latest Permian. Chinese Sciences Bulletin, 52(4): 512−520.

Wu, Y. S., Jiang, H. X., Yang, W., Fan, J. S., 2007b. Microbialite of anoxic condition from Permian−Triassic transition in Guizhou, China. Science in China Series D: Earth Sciences, 50(7): 1040−1051.

Wu, Y. S., Jiang, H. X., Fan, J. S., 2010. Evidence for sea-level falls in the Permian−Triassic transition in the Ziyun area, South China. Geological Journal, 45(2−3): 170−185.

Wu, Y. S., Yu, G. L., Li, R. H., Song, L. R., Jiang, H. X., Riding, R., Liu, L. J., Liu, D. Y., Zhao, R., 2014. Cyanobacterial fossils from 252 Ma old microbialites and their environmental significance. Scientific Reports, 4(3820): 1−5.

Xie, S. C., Pancost, R. D., Yin, H. F., Wang, H. M., Evershed, R. P., 2005. Two episodes of microbial change coupled with Permo/Triassic faunal mass extinction. Nature, 434(7032): 494−497.

Xu, G. R., Luo, X. M., Wang, Y. B., Zhou, L. Y., Xiao, S. Y., 1997. On a Building Model of Late Permian Reefs in Central Yangtze River Area. Wuhan: China University of Geosciences Press, 1−138 (in Chinese).

Yang, Z. Y., Wu, S. B., Yin, H. F., Xu, G. R., Zhang, K. X., Bi, X. M., 1991. Permo−Triassic Events of South China. Beijing: Geological Publishing House, 1−190 (in Chinese with English content and summary).

Yin, H. F., Zhang, K. X., Tong, J. N., Yang, Z. Y., Wu, S. B., 2001. The global stratotype section and point (GSSP) of the Permian−Triassic Boundary. Episodes, 24(2): 102−114.

Yin, H. F., Feng, Q. L., Lai, X. L., Baud, A., Tong, J. N., 2007. The protracted Permo-Triassic crisis and multi-episode extinction around the Permian−Triassic boundary. Global and Planetary Change, 55(1−3): 1−20.

Yu, J. X., Peng, Y. Q., Zhang, S. X., Yang, F. Q., Zhao, Q. M., Huang, Q. S., 2007. Terrestrial events across the Permian−Triassic boundary along the Yunnan−Guizhou border, SW China. Global and Planetary Change, 55(1−3): 193−208.

Zeeh, S., Becker, F., Heggemann, H., 2000. Dedolomitization by meteoric fluids: The Korbach fissure of the Hessian Zechstein basin, Germany. Journal of Geochemical Exploration, 69−70: 173−176.

Zhang, F., Feng, Q. L., Meng, Y. Y., He, W. H., Gu, S. Z., 2006. Stratigraphy of organic carbon isotope and associated events across the Permian−Triassic boundary in the Dongpan deep-water section in Liuqiao area, Guangxi, South China. Geoscience, 20(1): 42−48 (in Chinese with English abstract).

Zhao, L. S., Orchard, M. J., Tong, J. N., Sun, Z. M., Zuo, J. X., Zhang, S. X., Yun, A. L., 2007. Lower Triassic conodont sequence in Chaohu, Anhui Province, China and its global correlation. Palaeogeography, Palaeoclimatology, Palaeoecology, 252(1−2): 24−38.

Zhu, X. S., Wang, C. Y., Lü, H., Mu, X. N., Zhang, L. X., Qin, Z. S., Luo, H., Yang, W. R., Deng, Z. Q., 1994. Permian−Triassic boundaries in Jiangxi, China. Acta Micropalaeontologica Sinica, 11(4): 439−452 (in Chinese with English abstract).

(Edited by Xiu-Fang Hu)